

Study of a Miniature Air Bearing Linear Stage System

K. C. Fan^{1, a}, R. H. Yen^{2, b} and C. C. Ho^{3, c}

^{1,2} Department of Mechanical Engineering, National Taiwan University,
1, Sec. 4, Roosevelt Rd. 106, Taipei, Taiwan, ROC

³ASUSTeK Computer Inc., 150, Li-Te Rd., Peitou, Taipei, Taiwan, ROC

^afan@ntu.edu.tw, ^brhyen@ntu.edu.tw, ^cchichung_ho@asus.com.tw

Keywords: Air bearing, micro holes, Laser drilling, MEMS, straightness.

Abstract. For the purpose of micro stage used in micro positioning, a miniature aerostatic air bearing linear slide system was studied. Different arrayed micro-hole plates were fabricated. Using focused laser drilling, the diameter of the hole is limited to 300 μ m. However, with the MEMS process, smaller diameters up to 30 μ m could be achieved. A miniature air bearing linear slide was constructed by imbedding three developed air pads in the slider block, which could slide along a small granite straightedge to form a small sliding stage. The pressure distribution of air pad simulated by the Spectral Element Method was found in good agreement with experimental results. It was also found that the smaller the micro holes the better stability of the floating condition can be obtained. Straightness tests of the developed miniature air bearing sliding stage are carried out to show its feasibility.

Introduction

Air bearing type of linear stage is commonly adopted in precision stages due to its characteristics of no pollution, no sealing and cooling, and non-sticking motion. Through the designed groove pattern (or called the cavity pattern) and the drilled holes the air pad can eject distributed air pressure at the interface between the moving stage and the reference guide way and thus generate the aerostatic floating effect of the stage. The performance of air bearing stage is assessed by its floating stability due to the air hammering effect and its straightness along the motion. In the past, the technology of flatbed air bearing received broad attention and new products have been developed to improve the air bearing performance. Several approaches have been adapted to improve the stiffness and stability of flatbed air bearing, such as: add compensator or stabilizer such as damping cavity on air bearing [1, 2]; Change the surface profile of air bearing with grooved bearing [3], arc surface [4], conical shape [5, 6], or more complicated tri-conical gap-shaped holes [7]; and Change the bearing surface structure or use membrane type bearing [5, 8], or adapt porous material bearing [9, 10].

Due to the advent of micro/nano systems in recent years, many micro parts are transported by micro stages for fabrication, assembly, measurement, etc. Currently, most micro stages still use contact type linear bearing, which inevitably induces friction force and affects its micro/nano positioning control. The purpose of this study is to develop a miniature air bearing for micro stage and study its performance. The designed air bearing adopts multiple holes concept. The goals are to bring the pressure to extend location without using groove structure and maintain stable airflow effect. The diameter of the hole, number of holes and the corresponding fabrication process are to be considered for the performance assessment. The analytical result was compared with experimental data and validated on a linear sliding system.

Analysis and modeling

Fig. 1 shows a typical flatbed aerostatics air bearing. Theoretically, the airflow characteristic at air bearing and sliding guideway interface dominates the air bearing performance. Although the fly height of most air bearings is less than $20\mu\text{m}$, the continuous and laminar flow condition still validates [11]. The pressure distribution under the interface gap of each hole can be expressed by

$$\frac{\partial}{\partial x} \left(\frac{\rho h^3}{\mu} \frac{\partial P}{\partial x} \right) + \frac{\partial}{\partial y} \left(\frac{\rho h^3}{\mu} \frac{\partial P}{\partial y} \right) = 0 \quad (1)$$

where μ is the viscosity of the air and h indicates the height of the gap. The air pad design is shown in Fig. 2, which consists of a metal case, fabricated multi-hole thin plate, air pocket zone, inlet air socket and the supporting steel ball socket. Overall dimension is $24\text{mm} \times 20\text{mm}$. Using the mesh generation in association with Spectral Element Method [12] the air pressure distribution can be simulated. Fig. 3 plots an example of 25×25 evenly distributed holes with $300\mu\text{m}$ diameter each. It can be seen that the pressure is higher at the outlet of the hole than the flat bed position.

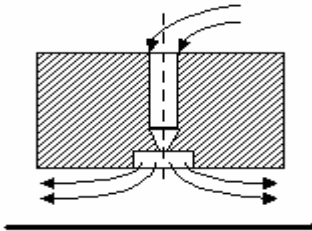


Fig. 1. Flatbed air bearing pad.

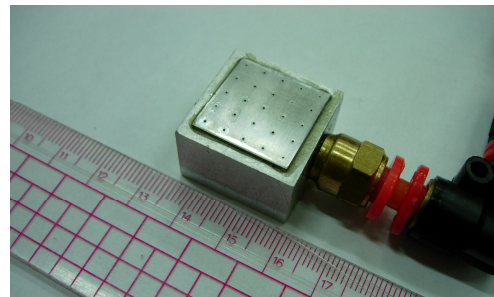


Fig. 4. Photo of a 25-hole air pad.

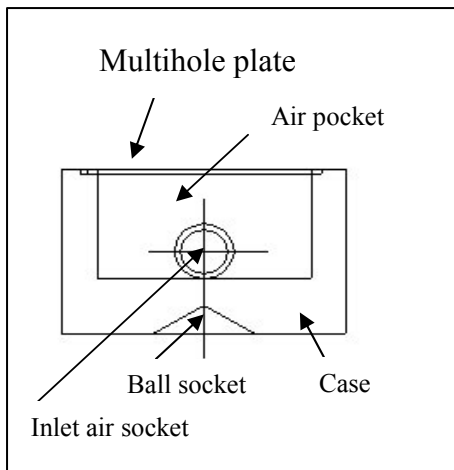


Fig. 2. Air pad design.

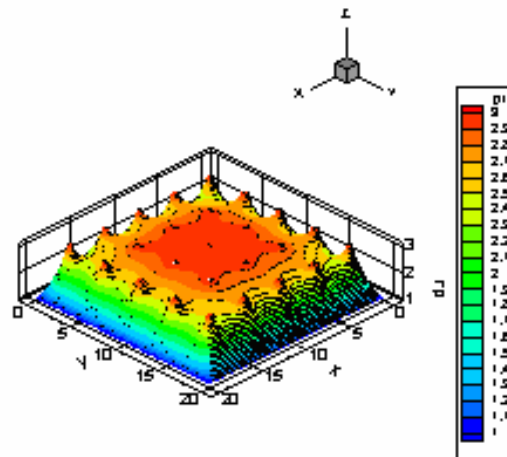


Fig. 3. Simulated air pressure distribution of 5×5 holes with $300\mu\text{m}$ dia. Each.

Micro air bearing fabrication

Laser drilling process. Micro-hole drilling is difficult to use traditional drilling process due to the limited drill size. A 400W Nd YAG laser drilling was firstly used on a thin metal plate of 1mm thickness. Due the limitation of the focus lens this study could only drill minimum diameter of $300\mu\text{m}$ of 25 uniformly distributed holes. Fig. 5 shows the photo of a packaged small air bearing pad. Due to the burning effect of the high temperature laser beam the circularity of the holes are apparently

irregular. Meanwhile, owing to the restriction of the focus lens, the minimum diameter of holes could only be as small as $100\mu\text{m}$. Some other methods for even smaller holes have to be studied.

MEMS process. The mask has to be produced for the MEMS process. Round shape hole was adopted in designing the mask. In this study, a (100) double side polished 4 inches silicon wafer of $500\mu\text{m}$ thickness was used to produce the mask. Using anisotropic etching to produce an (111) etching plane, the mask was designed to have 25 holes, 100 holes, and 400 holes, for the required hole diameters of $300\mu\text{m}$, $80\mu\text{m}$, and $30\mu\text{m}$ respectively, as shown in Fig. 3.

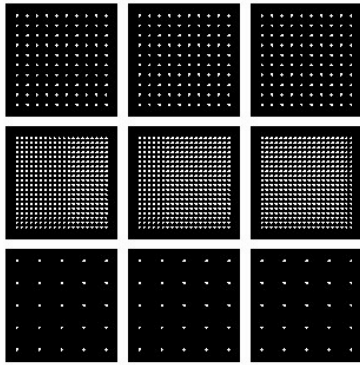


Fig. 5. Configuration of a 4'' Mask Design.

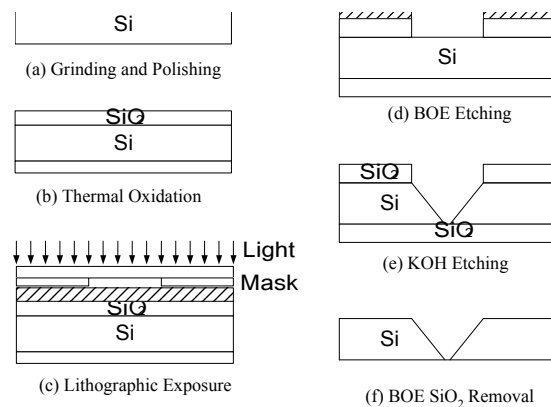


Fig. 6. MEMS fabrication processes.

The MEMS processes mainly consist of three steps, namely the SiO_2 growth, photoresist lithography and etching. As shown in Fig. 6, the silicon substrate needs to be ground and polished before growing a SiO_2 layer. Following the photoresist coating and the mask alignment, the lithography process can generate multi-hole pattern on the photoresist layer. The BOE etches the same pattern of holes on the SiO_2 layer. After removing the photoresist layer the KOH will etch tapered hole on the silicon substrate. Final process is to remove the SiO_2 layer with BOE etching. During the KOH wet etching process, the observed etching ratio on the (100) and (111) two planes is about 1:20. Therefore, to achieve a $30\mu\text{m}$ micro-hole outlet, the mask design was to have the inlet hole diameter of $670\mu\text{m}$. Other demanded sizes of the air pad micro holes should have the proportional hole diameters in the mask design.

Comparisons of analytical and experimental results of air pressure distribution

An air bearing pressure distribution measuring system was built to test the air bearing characteristics such as pressure distribution and stiffness. The testing structure needs to be able to sustain certain load. It also needs to have a moving platform with position control capability and pressure sensing device, as shown in Fig. 7. Fig. 8 shows the setup photo. The applied load can be adjusted to 4atm. Different air pads with number of holes in 25, 100 and 400; and hole sizes in $30\mu\text{m}$, $80\mu\text{m}$ and $300\mu\text{m}$ were tested. Fig. 9 shows an example of the measured pressure distribution on the line across the restrictors of an air pad having 25 holes with $300\mu\text{m}$ diameter each. Apparent spikes appear at the restrictor positions. Comparing to the simulated results as given in Fig. 3, Fig. 10 shows a quite good agreement of the pressure distribution across the holes. Fig. 11 shows the measured pressure distribution on the line across the restrictors of 100 holes with $80\mu\text{m}$ diameter, and Fig. 12 is for the 100 holes with $30\mu\text{m}$ diameter. It is apparent that the smaller the micro holes the better stability of the floating condition.

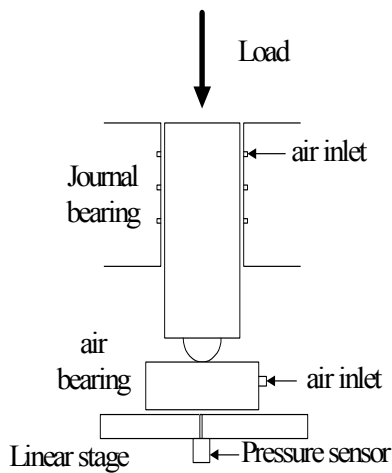


Fig. 7. Principle of air pressure testbed.

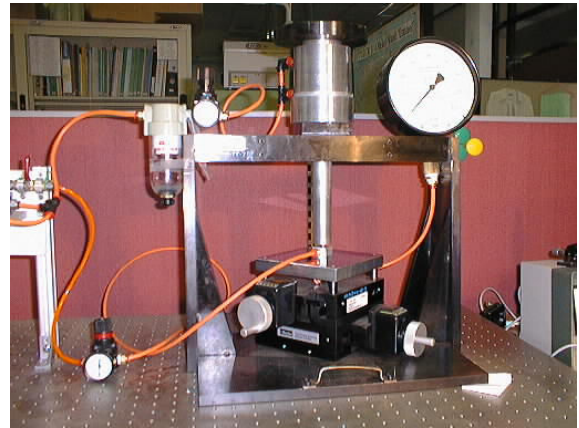


Fig. 8. Experimental setup.

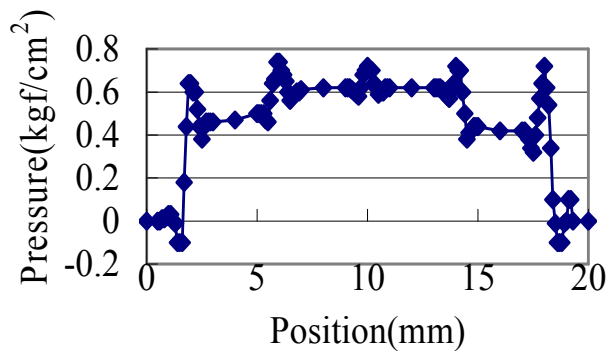


Fig. 9. Measured air pressure of 25x300µm pad.

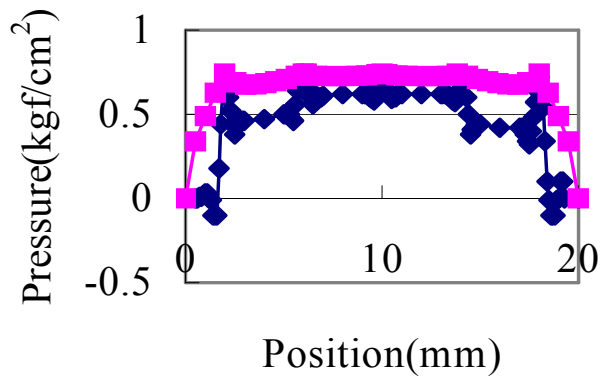


Fig. 10: Comparison of simulated and experimental results of 25x300µm pad.

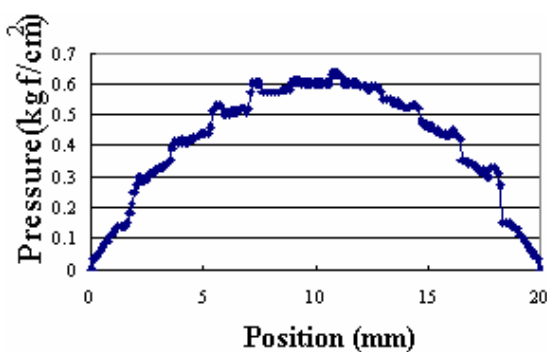


Fig. 11. Pressure distribution of 100hole/80µm pad.

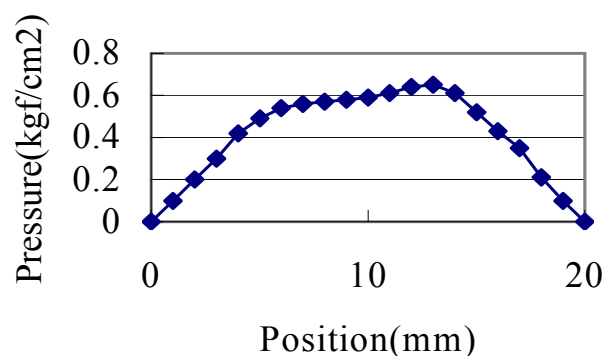


Fig. 12. Pressure curve of 100hole/30µm pad.

Straightness tests of the linear stage

With the assist of compressive airflow, the air bearing linear stage can travel along the guideway with frictionless contact. As this is a kind of surface support the effect of guideway surface roughness can be averaged out. Thus, the platform could move more smoothly. Using the designed air bearing and adopting the close weight balance type structure, an air bearing linear stage was developed as schematically shown in Fig. 13. A U-shape guide and six air bearings were assembled to form the sliding platform. The guideway was a class 1 granite straightedge. The motion straightness of the stage

was calibrated by the HP5529 laser Interferometer with its straightness module. As shown in Fig. 14, the measuring point is at the stage top while the air bearing support is located around the guideway. Any slight rotation of the stage due to the uneven air supply during the movement will create an Abbe' offset in the X direction at the measuring point. Fig. 15 shows the straightness errors in X direction along a 200mm motion, and Fig. 16 is the corresponding errors in Y direction. It is found that the Y-error is quite small while the X-error is relatively larger, which is quite in correspondence with the explanation in Fig. 12. It is also found that the smaller the micro holes the better the air pressure distribution, yielding to the better straightness motion of the linear stage.

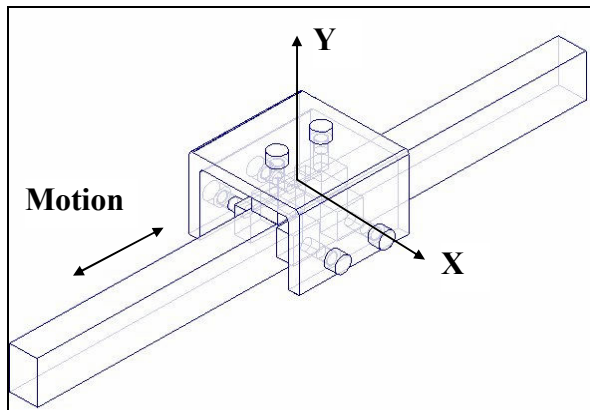


Fig. 13. Structure of miniature air bearing slide.

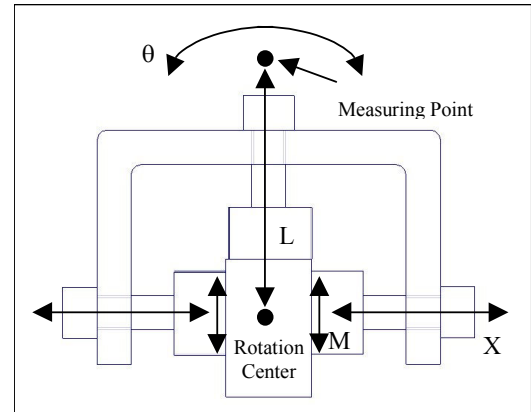


Fig. 14. Motion error cause by the stage rotation.

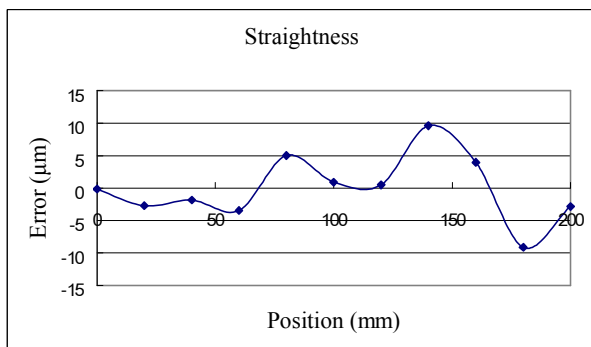


Fig. 15. Straightness error in X direction.

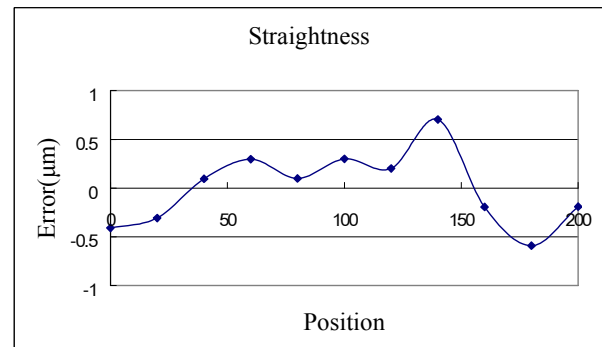


Fig. 16. Straightness error in Y direction.

Summary

In this research, a multiple micro holes air bearing and linear slide were developed. The air bearing pads were fabricated by using laser drilling and the modern MEMS technology. The multiple holes structure allows a better stability in airflow. Spectral Element Method was employed to analyze and simulate the pressure distribution of designed air bearing. The analytical result was in good agreement with experimental data. A granite straightedge was used to guide the moving table supported by the developed air bearing system. A laser interferometer system was used to assess the straightness performance of the stage. Although parameter identification and process control are very time consuming, the prototyped air bearing products exhibit good mechanical characteristics and performance.

Acknowledgments

The work reported forms part of a research program funded by the National Science Council of the Republic of China on the study of the Micro-CMM system.

References

- [1] Haruo, M. and Atsunobu, M., *J. Lubrication Technology*, Vol. 89 (1967), p. 283.
- [2] Stowell, T. B., *J. Lubrication Technology*, Vol. 93 (1971), p. 498.
- [3] Fuller, D. D., *Proc. of the 1st Int'l Gas Bearing Symposium*, Vol. 1 (1959).
- [4] Holster, P., Jacobs, J. and Roblee, *Transaction of the ASME*, Vol. 113 (1991), p. 768.
- [5] Bloudeel, E., Snoeys, R. and Devieze, L., *Proc. of the 7th Int'l Gas Bearing Symposium*, E2, (1976).
- [6] Plessers, P. and Snoeys, R., *Tribology*, Vol. 110 (1988), p. 263.
- [7] Wang, J. M., *Design of Gas Bearing System for Precision Application*, (Ph.D. Dissertation, Technical University Eindhoven, Netherlands 1993).
- [8] Holster, P. L. and Jacobs, J. A. H., *Tribology*, Vol. 20 (1987), p. 276.
- [9] Sneek, H. J., *J. Lubrication Technology*, Vol. 90 (1968), p. 804.
- [10] Sun, D. C., *J. Lubrication Technology*, Vol. 95 (1973), p. 457.
- [11] Gross, W. A., *Gas Film Lubrication*, (John Wiley & Sons, Inc. 1962).
- [12] Chen, X. W., *Application of Spectral Element Method in Flame Combustion*, (MS thesis, National Taiwan University, 1996).